The Quorum-Quenching Lactonase from *Bacillus thuringiensis* Is a Metalloprotein†

Pei W. Thomas,‡ Everett M. Stone,§ Alison L. Costello,|| David L. Tierney,|| and Walter Fast*,‡,§,⊥

Division of Medicinal Chemistry, College of Pharmacy, Graduate Programs in Biochemistry and Cell and Molecular Biology, and The Center for Molecular and Cellular Toxicology, The University of Texas at Austin, Austin, Texas 78712, and Department of Chemistry, University of New Mexico, Albuquerque, New Mexico 87131

Received January 10, 2005; Revised Manuscript Received March 28, 2005

ABSTRACT: Lactonases from *Bacillus* species hydrolyze the *N*-acylhomoserine lactone (AHL) signaling molecules used in quorum-sensing pathways of many Gram-negative bacteria, including *Pseudomonas aeruginosa* and *Erwinia carotovora*, both significant pathogens. Because of sequence similarity, these AHL lactonases have been assigned to the metallo-β-lactamase superfamily of proteins, which includes metalloenzymes of diverse activity, mechanism, and metal content. However, a recent study claims that AHL lactonase from *Bacillus* sp. 240B1 is not a metalloprotein [Wang, L. H., et al. (2004) *J. Biol. Chem. 279*, 13645]. Here, the gene for an AHL lactonase from *Bacillus thuringiensis* is cloned, and the protein is expressed, purified, and found to bind 2 equiv of zinc. The metal-bound form of AHL lactonase catalyzes the hydrolysis of *N*-hexanoyl-(*S*)-homoserine lactone but not the (*R*) enantiomer. Removal of both zinc ions results in loss of activity, and reconstitution with zinc restores activity, indicating the importance of metal ions for catalytic activity. Metal content, sequence alignments, and X-ray absorption spectroscopy of the zinc-containing lactonase all support a proposed dinuclear zinc binding site similar to that found in glyoxalase II.

Many Gram-negative bacteria use *N*-acylhomoserine lactone (AHL)[1] signaling molecules in intercellular communication pathways vital to their pathogenicity (*1*). AHL concentrations in culture media are thought to reflect cell density, and detection of these signals has been dubbed "quorum sensing" because they regulate various genes in a population-dependent manner, allowing bacteria to display a type of group behavior (*2*). For example, *Pseudomonas aeruginosa*, a human pathogen often found in lung infections of cystic fibrosis patients, relies on production of *N*-butanoyl-L-homoserine lactone (C4-HSL) and *N*-(3-oxododecanoyl)-L-HSL (3-oxo-C12-HSL) to regulate swarming, toxin and protease production, and proper biofilm formation (*3*); *Erwinia carotovora*, a plant pathogen responsible for soft rot, relies on production of *N*-hexanoyl-L-HSL (C6-HSL) to evade the plant's defense systems and to coordinate its production of pectate lyase during the infection process (*4*); AHL production is also linked to the pathogenicity of *Burkholderia mallei*, the etiologic agent of glanders, a biowarfare threat (*5*). Disrupting these intercellular quorum-sensing pathways is a significant therapeutic goal that has, not surprisingly, already been addressed by nature. Several naturally occurring "quorum-quenching" strategies have been discovered, including the biosynthesis of AHL antagonists and the expression of AHL degrading enzymes (*6*). One family of quorum-quenching enzymes, the AHL lactonases, hydrolyzes the lactone ring of a variety of AHL signals (Scheme 1) and has been shown to attenuate the swarming of *P. aeruginosa* (*7*), the infectivity of *E. carotovora* (*8*), and the quorum sensing of *Burkholderia thailandensis* (*9*).

Because of sequence similarity, the AHL lactonases have been assigned to the metallo-β-lactamase superfamily (*10*). This superfamily boasts a diverse set of proteins with examples of no-metal, mononuclear zinc, dinuclear zinc, zinc/iron, and dinuclear iron active sites and shows considerable diversity in catalytic activity and mechanism (*11*). The determinants of metal binding affinity and specificity are often complex and cannot be predicted solely from sequence data. Thus far, all of the known hydrolytic enzymes found in this protein superfamily rely on one or two metal ions for catalysis, but a recent report has made the interesting claim

† This research was supported by a National Institutes of Health Research Scholar Development Award (K22 AI50692) to W.F. from the National Institute of Allergy and Infectious Diseases and by the Robert A. Welch Foundation (F-1572) to W.F. Mass spectra were acquired in the CRED Analytical Core supported by NIEHS Grant ES07784. The National Synchrotron Light Source is supported by the U.S. Department of Energy.

* To whom correspondence should be addressed at the College of Pharmacy, PHAR-MED CHEM, The University of Texas at Austin, 1 University Station, A1935, Austin, TX 78712. Phone: (512) 232-4000. Fax: (512) 232-2606. E-mail: WaltFast@mail.utexas.edu.

‡ Division of Medicinal Chemistry, The University of Texas at Austin.

§ Graduate Program in Cell and Molecular Biology, The University of Texas at Austin.

|| University of New Mexico.

⊥ Graduate Program in Biochemistry and The Center for Molecular and Cellular Toxicology, The University of Texas at Austin.

[1] Abbreviations: AHL, *N*-acylhomoserine lactone; HSL, homoserine lactone; MALDI-TOF, matrix-assisted laser desorption−ionization time of flight; LB, Luria−Bertani; PCR, polymerase chain reaction; SDS, sodium dodecyl sulfate; PAGE, polyacrylamide gel electrophoresis; OD_{600}, optical density at 600 nm; ICP-MS, inductively coupled plasma mass spectrometry; *aiiA*, the gene for AHL lactonase; bp, base pairs; equiv, equivalents; TEV, tobacco etch virus; TB, Terrific broth; MWCO, molecular weight cutoff; HIC, hydrophobic interaction chromatography; ESI-HRMS, electrospray ionization high-resolution mass spectrometry; TLC, thin-layer chromatography; mS, millisiemens; BGSC, *Bacillus* genetic stock center; EXAFS, extended X-ray absorption fine spectroscopy.

10.1021/bi050050m CCC: $30.25
Published on Web 04/30/2005

Scheme 1

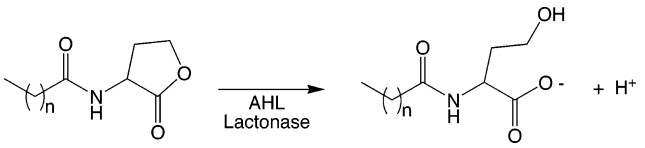

that AHL lactonases are *not* metalloproteins (*12*). In contrast, this study presents, to our knowledge, the first evidence that the AHL lactonase from *Bacillus thuringiensis* is, in fact, a stereospecific metalloprotein. The 2 equiv of zinc that can bind to this enzyme are found to be essential for catalytic activity and are bound in close proximity, forming a dinuclear site.

MATERIALS AND METHODS

Cloning of the AHL Lactonase Coding Sequence. Genomic DNA was isolated from a culture of *B. thuringiensis* 4A3 [*Bacillus* Genetic Stock Center (BGSC), Columbus, OH] according to published procedures (*13*). Using primers and PCR conditions described by Dong et al. (*14*), the coding sequence for AHL lactonase (*aiiA*) followed by a short extension was amplified, ligated into a pGEM-T vector (Promega, Madison, WI), and used to transform *Escherichia coli* DH5αE cells. The forward primer used was 5′-ATGGGATCCATGACAGTAAAGAAGCTTTAT-3′, and the reverse primer, containing an *Eco*RI restriction site (underlined), was 5′-GTCGAATTCCTCAACAAGATACTC-CTAATG-3′. The resulting plasmid was purified (QIAprep; Qiagen, Valencia, CA) and used as a template in a PCR to incorporate an *Xmn*I restriction site (underlined; see below) immediately before the ATG codon by using the same reverse primer noted above and a forward primer obtained from Sigma-GENOSYS (The Woodlands, TX), 5′-CGG-GAAGGATTTCAATGACAGTAAAGAAGCTTTAT-3′, and a temperature program of 5 min at 95 °C followed by 30 cycles of 30 s at 95 °C, 30 s at 55 °C, and 75 s at 72 °C. The resulting product was gel purified (Qiaquick; Qiagen), and this product and the expression vector pMAL-c2X (New England Biolabs, Beverly, MA) were digested using *Xmn*I and *Eco*RI, purified (Qiaquick; Qiagen), ligated together to form pMAL-aiiA, and used to transform *E. coli* DH5αE cells for amplification and sequencing.

Introduction of a TEV Protease Cleavage Site into pMAL-aiiA. The oligonucleotide 5′-aacctcgggGAAAACCTG-TATTTTCAGGGAaggatttcaatgaca-3′ (Sigma-GENOSYS) was used to change the protease cleavage site between the N-terminal maltose-binding protein and the C-terminal AHL lactonase as follows. This primer contains an *Ava*I restriction site (underlined) followed by 21 nucleotides corresponding to the coding sequence for the tobacco etch virus (TEV) protease recognition site (upper case). The 9 bases 5′ and the 15 bases 3′ to the TEV coding sequence are homologous to the pMAL-c2X multiple cloning site and the first two codons of *aiiA*. Using pMAL-aiiA as a template, the TEV primer above as the forward primer, and the original reverse primer, a PCR was carried out using an MJ Research PTC 200 thermocylcer (Waltham, MA) and Triplemaster PCR reagents (Eppendorf, Westbury, NY). The resulting product was purified (Qiaquick; Qiagen), and both the PCR product and pMAL-c2X were digested with *Ava*I and *Eco*RI. The resulting fragments were purified (Qiaquick; Qiagen) and ligated together using T4 DNA ligase (Fisher, Pittsburgh, PA) to form pMAL-t-aiiA, which was subsequently used to transform *E. coli* DH5αE cells. The *aiiA* coding sequence in pMAL-t-aiiA was completely sequenced at the DNA Facility (The University of Texas at Austin) and indicated that there were no undesired mutations.

Expression and Purification of MBP-AHL Lactonase. E. coli DH5αE cells harboring pMAL-t-aiiA were incubated at 37 °C with shaking in Terrific broth (TB) supplemented with 0.2% glucose, 1 mM $ZnSO_4$ (in initial experiments, this zinc supplement was omitted), and 50 μg/mL ampicillin. Expression of recombinant MBP-AHL lactonase fusion protein was induced upon addition of 0.3 mM IPTG after cells reached an OD_{600} of 0.5−0.7, and expression was continued for an additional 16 h at 25 °C. Cells were harvested by centrifugation, washed with 20 mM Tris-HCl buffer and 200 mM NaCl, pH 7.4, and stored at −20 °C until use.

Purification of the MBP-AHL Lactonase Fusion Protein. All purification procedures were done at 4 °C unless otherwise specified. Chromatographic procedures were performed using a BioLogic LP protein purification system (Bio-Rad, Hercules, CA). On ice, cell pellets from 1 L were suspended in 100 mL of column buffer (20 mM Tris-HCl buffer, 200 mM NaCl, pH 7.4) and sonicated with for pulses of 30 s each with 120 s cooling intervals. Cell debris was removed by centrifugation at 34500*g* for 30 min. The protein concentration of the resulting supernatant was determined using the Bio-Rad protein assay kit (Bio-Rad), calibrated with bovine serum albumin (BSA) as the standard. The supernatant was subsequently diluted to 1.5 mg/mL with column buffer, made 2 mM in DTT, and loaded onto a 2.5 × 20 column of amylose−agarose resin (New England Biolabs) at a flow rate of 1.0 mL/min. After being washed with 10−12 column volumes of column buffer, the fusion protein was eluted with 10 mM maltose and 2 mM DTT in column buffer. The eluted fractions containing fusion protein were transferred into Spectra/Por dialysis tubing with a molecular mass cutoff (MWCO) of 12000−14000 Da (Spectrum Laboratories, Rancho Dominguez, CA) and dialyzed overnight against buffer A (20 mM Tris-HCl buffer, pH 7.4, 5 mM NaCl) and 2 mM DTT at 4 °C. The dialyzed protein was applied to a DEAE-Sepharose FF column (1.5 × 15 cm) equilibrated with buffer A and washed with 200 mL of buffer A made to 160 mM NaCl, and then fractions were collected while varying the NaCl concentrations from 160 to 250 mM. The active fraction of the MBP-AHL lactonase fusion protein was eluted at a conductivity near 19 mS/cm (approximately 180−190 mM NaCl), and the remaining proteins including apo MBP-AHL lactonase were eluted at higher salt concentrations with a conductivity near 26 mS/cm. Salt gradients were often adjusted manually to optimize separation between peaks.

Specific Proteolysis of MBP-AHL Lactonase and Subsequent Purification of Untagged AHL Lactonase. The fractions containing active MBP-AHL lactonase were concentrated using an Amicon Ultra-15 (10000 MWCO) centrifugal filter device (Millipore, Billerica, MA) to approximately 1 mg/mL. During this concentration step, the final sample was made 50 mM in Tris-HCl buffer, pH 8, 160 mM in NaCl, 1 mM in DTT, and 4% (w/w) in TEV protease (*15*, *16*). Specific proteolysis of MBP-AHL lactonase was carried out

at 10 °C for 16−20 h with slow gentle shaking. Reaction products were characterized by SDS−PAGE, and the site of proteolysis was verified by N-terminal sequencing of the final protein at the Protein Facility (The University of Texas at Austin).

The protein cleavage products were diluted with an equal volume of buffer A and applied to a DEAE-Sepharose FF column (1.5 × 10 cm). The MBP fragment and TEV protease both were eluted from the column using 160 mM NaCl in buffer A. Untagged AHL lactonase was later eluted using 170 mM NaCl in buffer A. To remove any trace amounts of uncleaved MBP-AHL lactonase still remaining, the eluate was reloaded onto a small amylose−agarose affinity column (1.5 × 10 cm), and untagged AHL lactonase was collected in the flow-through and wash fractions.

Additional Purification Steps, Final Dialysis, and Metal Analysis. During some preparations, AHL lactonase showed minor degradation products that could be removed by using *tert*-butyl hydrophobic interaction chromatography (HIC). If required, a sample was made 2 M in ammonium sulfate and loaded onto a *tert*-butyl HIC column (2.5 × 5 cm) preequilibrated with buffer B [25 mM Tris-HCl, pH 7.4, and 2 M $(NH_4)_2SO_4$]. After being washed with buffer B, purified AHL lactonase was eluted using a 200 mL decreasing linear gradient from 2 to 1.6 M $(NH_4)_2SO_4$. Fractions containing purified AHL lactonase, as judged by SDS−PAGE and activity, were pooled and dialyzed as described below.

As a final purification step for all forms of AHL lactonase, extraneously bound metals were removed from MBP-AHL lactonase by dialysis against Chelex-100 (Bio-Rad) treated 5 mM NaCl and 20 mM Hepes buffer, pH 7.4. The resulting protein was concentrated using an Amicon Ultra-15 centrifugal filter device and made 10% in glycerol before it was frozen in aliquots (using liquid N_2) and stored at −80 °C.

To determine final metal content, protein samples and associated dialysis buffers were analyzed by inductively coupled plasma mass spectrometry (ICP-MS; Department of Geological Sciences, The University of Texas at Austin) by subtracting the concentration of zinc found in dialysis buffers from the zinc concentrations of the protein samples and dividing by the proteins' concentrations.

Preparation of Apo MBP-AHL Lactonase. All of the buffers used for the following steps were treated to remove trace metals by using Chelex-100 according to the manufacturer's protocols (Bio-Rad), and plasticware was used whenever possible. Fractions from the DEAE column that contained active AHL lactonase activity were pooled and dialyzed against two changes of 40 volumes of 2 mM 1,-10-phenanthroline in 20 mM Hepes buffer containing 5 mM NaCl and 2 mM DTT, pH 7.0, over a 40 h period. Dialysis against 1,10-phenanthroline was found to be more effective at removing zinc from purified enzyme than EDTA (data not shown). Native PAGE can monitor removal of metals because apo and metal-bound AHL lactonase have different mobilities (see below). To remove small amounts of any protein after dialysis that still retained metal ions, the dialyzed sample was then applied to a DEAE-Sepharose FF column (1.5 × 10 cm), which was equilibrated in dialysis buffer containing 1,10-phenanthroline (2 mM). After being extensively washed with Chelex-100 treated buffer C (20 mM Hepes, 5 mM NaCl, pH 7.4), the apoenzyme was specifically eluted using a salt gradient as described above. The peak containing inactive apoprotein was pooled and dialyzed overnight against buffer C containing 1,10-phenanthroline (2 mM) and DTT (2 mM), and then the 1,10 phenanthroline was removed either by dialysis or by repeated washing with buffer C and DTT (2 mM) in an Amicon Ultra-15 centrifugal filter device.

Reconstitution of Zinc-Containing MBP-AHL Lactonase from Apoprotein. To reincorporate zinc, the apoprotein was dialyzed against buffer C containing 2 mM $ZnSO_4$, pH 7.1, for 8 h. Excess Zn(II) was subsequently removed by overnight dialysis against buffer C containing 2 mM DTT. Reincorporation of zinc is not an efficient process under these conditions. So, to remove any remaining apoprotein before the reconstituted metalloprotein was characterized, the reconstitution mixtures were applied to a DEAE-Sepharose FF column (1 × 10 m) equilibrated with buffer C, and active MBP-AHL lactonase that had reincorporated zinc was separated from any remaining apoprotein as described above. The resulting reconstituted metalloprotein was dialyzed against Chelex-100 treated buffer C before metal analysis and activity tests to remove any extraneously bound metal ions.

Native and SDS−PAGE Characterization of Protein Samples. SDS−PAGE (*17*) was conducted using a 4% stacking gel and 12% separating gel at room temperature for 40 min at 200 V. Native PAGE gels contained the same reagents except that SDS and DTT were omitted, and samples were subjected to electrophoresis for 100 min at 12 mA at 4 °C. Gels were all stained using Pierce GelCode Blue stain reagent (Rockford, IL).

Mass Spectral Analysis of Products Formed in the AHL Lactonase Reaction. In 1.5 mL microcentrifuge tubes, *N*-hexanoyl-(*R*,*S*)-homoserine lactone (racemic C6-HSL, 20 mM) (Fluka, Milwaukee, WI) was incubated overnight at 25 °C with 150 nM AHL lactonase in 20 mM Tris-HCl buffer, pH 7.6. Control samples were also prepared by omitting the enzyme from the incubation mixture. Reactions were desalted on a protein trap (Protein MicroTrap; Michrom, Auburn, CA) and analyzed by electrospray ionization mass spectrometry (ESI-MS) on a ThermoFinnigan LCQ ion trap spectrometer as described previously (*18*).

*Synthesis of N-Hexanoyl-(S)-homoserine Lactone [C6-(S)-HSL] (**1**).* All synthetic reagents were purchased from Sigma-Aldrich Chemical Co. (St. Louis, MO). In a procedure similar to that of Chhabra et al. (*19*), triethylamine (23 mmol) was added to a stirred suspension of (*S*)-α-amino-γ-butyrolactone hydrobromide (10 mmol) in dimethylformamide (24 mL) at 0 °C. Hexanoyl chloride (14 mmol) was added dropwise, and the reaction was allowed to come to room temperature with continued stirring for 2 h. Solvent was removed by rotary evaporation with heating at ≤40 °C. The residue was dissolved in CH_2Cl_2 and washed sequentially with 1 M Na_2SO_4 solution (3 × 20 mL) and saturated NaCl solution (1 × 20 mL). The organic layer was dried over anhydrous $MgSO_4$, and solvents were removed by rotary evaporation. The final compound was further purified either by recrystallization from ethyl acetate and petroleum ether or by column chromatography on silica gel using ethyl acetate as the mobile phase. The product was obtained in 60% yield: $R_f = 0.50$ in ethyl acetate; $T_m = 133-136$ °C (uncorrected); ^{1}H NMR (300 MHz, $CDCl_3$) δ 0.90 (t, 3 H), 1.29−1.35 (m, 4 H), 1.61−1.71 (m, 2 H), 2.06−2.18 (m, 1 H), 2.21−2.28

(m, 2 H), 2.82−2.91 (m, 1 H), 4.25−4.34 (m, 1 H), 4.47 (d, 1 H), 4.51−4.60 (m, 1 H), 6.06 (s, 1 H); ^{13}C NMR (75 MHz, $CDCl_3$) 14.15, 22.60, 25.35, 30.91, 31.60, 36.40, 49.50, 66.36, 174.01, 175.83; EI-HRMS MH^+_{calc} = 200.1287, MH^+_{obs} = 200.1293; $[\alpha]^{20°C}_{D,methanol}$ = −29.4°.

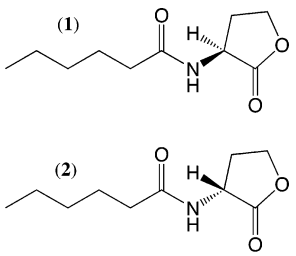

Synthesis of N-Hexanoyl-(R)-homoserine Lactone [C6-(R)-HSL] (2). The (*R*) enantiomer was synthesized in a procedure similar to that for synthesis of the (*S*) enantiomer, except that (*R*)-α-amino-γ-butyrolactone hydrochloride was used as a starting material and resulted in a 22% yield: R_f = 0.83 in ethanol; T_M = 133−135 °C (uncorrected); ^{1}H NMR (300 MHz, $CDCl_3$) δ 0.87 (t, 3 H), 1.26−1.31 (m, 4 H), 1.59−1.67 (m, 2 H), 2.08−2.15 (m, 1 H), 2.19−2.24 (m, 2 H), 2.81 (m, 1 H), 4.21−4.30 (m, 1 H), 4.41−4.47 (t, 1 H), 4.50−4.59 (m, 1 H), 6.16 (s, 1 H); ^{13}C NMR (75 MHz, $CDCl_3$) 13.87, 22.31, 25.10, 30.50, 31.31, 36.40, 49.15, 66.09, 173.78, 175.65; EI-HRMS MH^+_{calc} = 200.1287, MH^+_{obs} = 200.1295; $[\alpha]^{20°C}_{D,methanol}$ = +28.2°.

Kinetic Assay of AHL Lactonase Activity. Hydrolysis of AHLs yields a ring-opened product and, at pH values above the pK_a of the product's carboxylic acid, one proton (Scheme 1). Net production of protons can be detected by using a continuous spectrophotometric pH indicator assay that was originally reported for measuring carbonic anhydrase and haloalkane dehalogenase activity (*20*−*22*). Briefly, reactions are weakly buffered, and a colorimetric pH indicator with a pK_a similar to the reaction pH is added, becoming part of the buffering system. Any net change in proton concentration will alter the indicator's protonation state and result in a color difference that can be quantified using a standard curve. A typical assay contains 700 μL of deionized water, 750 μL of 2× dye solution (2 mM buffer, 0.2 M Na_2SO_4, and indicator), 20 μL of enzyme, and 30 μL of 0.5 M substrate dissolved in methanol. Particular buffers and indicators must be chosen as pairs to match the reaction pH and indicator pK_a. The concentrations of the indicators were adjusted experimentally to yield a final assay solution with an absorbance of 1.0 at the desired wavelength (557 nm for phenol red). The indicator/buffer pair 40 μM phenol red/1 mM Hepes was often used for reactions monitored at pH 7.4−7.6, although different indicator/buffer pairs can be chosen for other pH ranges (*21*). Initial rates of AHL hydrolysis were measured as a decrease in absorbance at 557 nm over 1 min at 28 °C. Observed rates were corrected for background hydrolysis of AHLs by substituting 20 μL of storage buffer for the enzyme stock and subtracting the observed rate from incubations including enzyme. A standard curve of absorbance changes due to addition of known amounts of HCl (2.0 N standard from Sigma-Aldrich) is constructed and used to convert the observed change in absorbance during enzymic reactions to a change in the proton concentration.

EXAFS of MBP-AHL Lactonase. Samples of MBP-AHL lactonase (1 mM) containing 2 equiv of zinc were prepared in Chelex-100 treated buffer C with 10% (v/v) glycerol added as a glassing agent. Samples were loaded in Lucite cuvettes with 6 μm polypropylene windows and frozen rapidly in liquid nitrogen. X-ray absorption spectra were measured at the National Synchrotron Light Source (NSLS), beamline X9B, with a Si(111) double crystal monochromator; harmonic rejection was accomplished using a Ni focusing mirror. Fluorescence excitation spectra for all samples were measured with a 13-element solid-state Ge detector array. The detectors were run at a total incident count rate (ICR) of <100 kHz per channel, with fluorescence count rates (K_α) ∼ 1.1 kHz per channel. Samples were held at ∼15 K in a Displex cryostat during XAS measurements. EXAFS spectra were measured with 10 eV steps below the edge, 0.5 eV steps in the edge region, and 0.05 Å^{-1} steps in the EXAFS region. Integration times varied from ∼1 s in the preedge region to 15 s at $k \approx 14$ Å^{-1} for a total integration time of approximately 45 min per scan. X-ray energies were calibrated by reference to the absorption spectrum of the appropriate metal foil, measured concurrently with the protein spectra. The first inflection point of the metal foil was assigned as the Zn K_α binding energy, 9659 eV.

Data were processed using the program SixPack, available free of charge from http://www-ssrl.slac.stanford.edu/∼swebb/index.htm. All fluorescence and ICR data were examined prior to averaging to confirm the absence of artifacts. Data were measured in duplicate on two samples from independent purifications; fits to the two data sets were equivalent. The spectra in Figure 4 represent the average of the two data sets (15 total scans, 13 detector channels per scan). Background subtraction was accomplished with a Gaussian fit to the preedge region, centered near the K_α fluorescence energy, and a three-region spline of fourth order in the EXAFS region. Data were converted from energy to *k*-space using $k = [2m_e(E - E_0)/h^2]^{1/2}$ with E_0 set at 9680 eV. Resultant EXAFS spectra were Fourier transformed over the range k = 1−13.6 Å^{-1}. The first shell (ΔR = 0.8−2.0 Å) was reverse Fourier transformed over the same *k*-range, ca. 10 deg of freedom (degrees of freedom = $N_{pts} - N_{var}$, where $N_{pts} = 2\Delta k \Delta R/\pi + 2$) (*23*). The Fourier filtered first shell EXAFS were fit to eq 1 using the nonlinear least-squares engine of IFEFFIT that is distributed with SixPack (IFEFFIT is open source software available from http://cars9.uchicago.edu/ifeffit):

$$\chi(k) = \sum \frac{N_{as} A_s(k) S_c}{k R_{as}^2} \exp(-2k^2 \sigma_{as}^2) \times \exp(-2R_{as}/\lambda) \sin[2kR_{as} + \phi_{as}(k)] \quad (1)$$

where N_s is the number of scatterers within a given radius (R_{as}, ± σ_{as}), $A_s(k)$ is the backscattering amplitude of the absorber−scatterer (as) pair, S_c is a scale factor, $\phi_{as}(k)$ is the phase shift experienced by the photoelectron, λ is the photoelectron mean free path, and the sum is taken over all shells of scatterering atoms included in the fit. Theoretical amplitude and phase functions, $A_s(k)\exp(-2R_{as}/\lambda)$ and $\phi_{as}(k)$, were calculated using FEFF version 8.00 (*24*). The Zn−N scale factor, S_c in eq 1, and the threshold energy, ΔE_0, were determined by fitting the experimental spectrum for

tetrakis(1-methylimidazole)zinc(II) perchlorate, $Zn(MeIm)_4$ (*25*). The optimal values found were $S_c = 0.78$ and $\Delta E_0 = -21$ eV. Fits to protein data were then obtained for all reasonable coordination numbers, holding S_c and ΔE_0 constant, while varying R_{as} and σ_{as}^2. Multiple scattering contributions from histidine ligands were approximated by fitting FEFF calculated paths to the experimental EXAFS data for $Zn(MeIm)_4$ (*25*). Best fits resulted in four prominent multiple scattering features, representing 140 total paths. Paths of similar overall length were combined to match these four prominent features. Consequently, the labels in Table 2, while reflecting the greatest contributor to a combined path, are nonphysical. These combined paths were used to fit protein data, fixing the number of imidazole ligands per zinc ion at half-integral values while varying R_{as} and σ_{as}^2 (Table 2). Each imidazole ligand was treated as a fixed unit, maintaining the relative C−C and C−N distances throughout the fit. Metal−metal (Zn−Zn) scattering was modeled by fitting calculated amplitude and phase functions to the experimental EXAFS of $Zn_2(sapln)_2$.

RESULTS

Cloning of pMAL-t-aiiA. The sequence specifically amplified from *B. thuringiensis* (BGSC 4A3) matches the sequence reported for the AHL lactonase from *B. thuringiensis* subsp. kurstaki (accession number AF478059) (*14*, *26*) and is followed by an additional 146 nucleotides of noncoding sequence that extend after the stop codon. After cloning of this insert into a pMAL-c2X vector, initial expression and cleavage experiments indicated that specific proteolysis of the linker between MBP and AHL lactonase by factor Xa was not efficient and resulted in significant loss of AHL lactonase activity. To optimize this cleavage step, the protease cleavage site was mutated to a sequence coding for the TEV protease cleavage site, ENLYFQ↓G, followed by three extra amino acids (RIS) that result from retaining an *Xmn*I site in the vector to facilitate subcloning. TEV protease recognizes a specific sequence and works efficiently at 4−10 °C, which are both important features for optimizing this step of AHL lactonase purification (*16*).

Purification of Active MBP-AHL Lactonase. The MBP-AHL lactonase fusion protein was purified to >95% homogeneity by two chromatographic steps, an amylose affinity column and a DEAE anion-exchange column (Figure 1). After the initial affinity column purification, the protein appeared to be nearly homogeneous when visualized by SDS−PAGE, but native PAGE revealed two major species (see below). These two species could be separated by anion-exchange chromatography into an active peak that eluted at a conductivity near 19 mS/cm and an inactive peak that eluted near 26 mS/cm (Figure 2). The N-terminal sequence of the inactive peak was determined to be MKIEEGKLVIW, confirming that this protein contains an N-terminal MBP fusion. For study of the active protein, dialysis of the fusion protein found in the active peak against Chelex-100 treated buffer resulted in purified MBP-AHL lactonase that was used for functional studies. Typical yields were 30 mg of purified fusion protein from 2 L of expression culture.

Purification of Untagged AHL Lactonase. MBP-AHL lactonase was treated with TEV protease to cleave the linker between MBP and AHL lactonase. After digestion, three

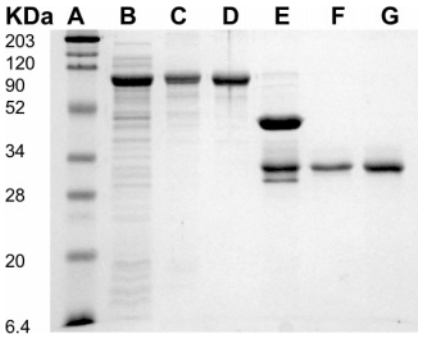

FIGURE 1: Purification of AHL lactonase. 12% SDS−PAGE denaturing protein gel showing proteins from (A) MW markers, (B) crude soluble extract, (C) eluate from agarose affinity column, (D) eluate from DEAE anion-exchange column, (E) after cleavage by TEV protease, (F) after DEAE chromatography, and (G) after amylose affinity chromatography.

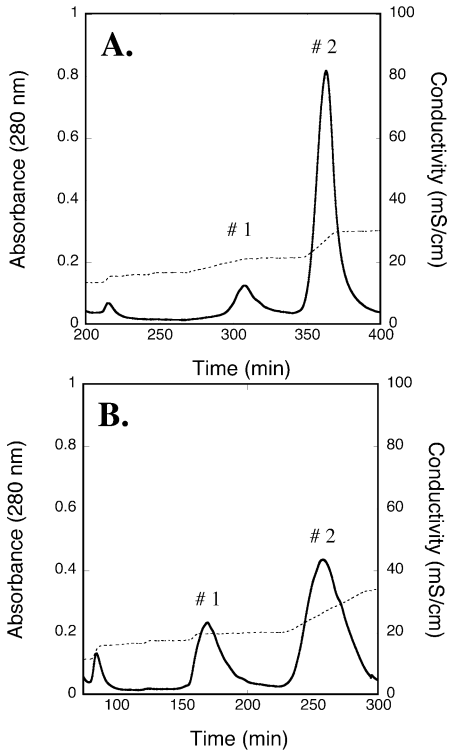

FIGURE 2: Apo and 2 equiv of zinc-containing MBP-AHL lactonases are separated by ion-exchange chromatography. Solid lines show absorbance at 280 nm. Dashed lines show conductivity. (A) Initial DEAE column chromatography after growth in TB media. (B) Initial DEAE column chromatography after growth and expression in TB media and 1 mM $ZnSO_4$. In both cases, peak 1 contains active MBP-AHL lactonase that contains 2 equiv of zinc and peak 2 contains apoprotein. Retention times are somewhat different because salt concentrations were adjusted manually.

major components were detected using SDS−PAGE that approximately correspond to the molecular masses expected for MBP (42 kDa), untagged AHL lactonase (29 kDa), and TEV protease (28 kDa) (Figure 1). Both MBP and TEV protease were removed during DEAE-Sepharose chromatography, and a small amylose−agarose affinity column removed any uncleaved MBP-AHL lactonase that remained. This procedure typically results in a yield of 9 mg of purified untagged AHL lactonase from 2 L of expression culture. The N-terminal sequence of purified AHL lactonase was determined to be GRISMTVK, confirming that TEV protease cleaved at the expected site.

Table 1: Zinc Content and Steady-State Rate Constants of Various AHL Lactonase Preparations for Hydrolysis of C6-(*S*)-HSL (**1**)[a]

	equiv of zinc	k_{cat} (s^{-1})	K_M (mM)	k_{cat}/K_M ($s^{-1}\,M^{-1}$)
MBP-AHL lactonase (TB)	1.6	107 ± 3	6.4 ± 0.4	17000 ± 2000
MBP-AHL lactonase (TB + $ZnSO_4$)	2.3	102 ± 3	5.4 ± 0.4	19000 ± 2000
MBP-AHL lactonase (apo)	0.1	–[b]	–	–
MBP-AHL lactonase (apo + $ZnSO_4$)	2.5	70 ± 3	6.3 ± 0.6	11000 ± 2000
AHL lactonase (MBP removed)	1.7	117 ± 5	6.7 ± 0.6	17000 ± 2000

[a] Reactions are carried out at 28 °C and pH 7.4. [b] Apo MBP-AHL lactonase retains <3% of the activity of the dinuclear zinc forms.

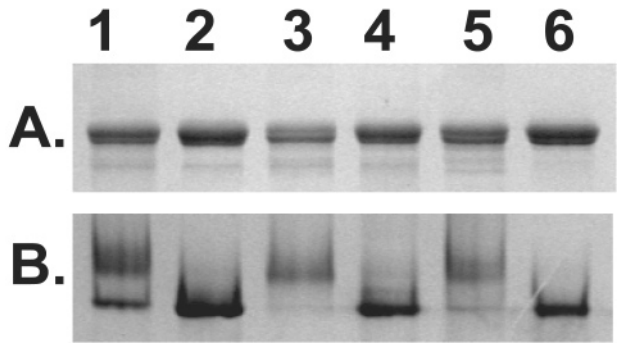

FIGURE 3: PAGE characterization of AHL lactonase preparations. (A) 12% denaturing SDS−PAGE gel. (B) 12% native PAGE gel. Lanes are the same in both. (1) Protein mixture after initial affinity purification. (2) Peak 1 from DEAE column. (3) Peak 2 from DEAE column. (4) MBP-AHL lactonase containing 2 equiv of zinc. (5) Apo MBP-AHL lactonase. (6) Apo-MBP-AHL lactonase after reconstitution with zinc.

Metal Analysis of MBP-AHL Lactonase and Untagged AHL-Lactonase. The molar ratios of purified MBP-AHL lactonase and untagged AHL lactonase to zinc were determined to be 1.6 and 1.7 equiv, respectively, indicating that this enzyme may be capable of binding 2 equiv of zinc per protein monomer (Table 1). During protein expression, if the growth media are supplemented with $ZnSO_4$ (1 mM), then the amount of active protein eluted in the first peak (~19 mS) from the DEAE column was significantly increased (Figure 2), and the resulting purified MBP-AHL lactonase is then isolated with 2.3 equiv of tightly bound zinc (Table 1). Purified MBP-AHL lactonase containing 2 equiv of zinc was found to elute at the same conductivity as this first peak (data not shown) and also has the same mobility as this first peak when characterized by native PAGE (Figure 3). The largest source of error in determining the equivalents of zinc can be attributed to the measurement of accurate protein concentrations and results in an approximate 10% error when using a Bradford-based assay (*27*). Two other protein concentration assays, the bicinchoninic acid (BCA) method (*28*) and a calculated extinction coefficient at 280 nm (*29*), were compared with the Bradford method and indicate slightly higher protein concentrations. These differences are less than 30% and still indicate that 1.7−1.9 equiv of zinc is bound to MBP-AHL lactonase purified from $ZnSO_4$-supplemented growth media.

Preparation of Apo MBP-AHL Lactonase. Extensive dialysis of MBP-AHL lactonase against a zinc chelator, *o*-phenanthroline, followed by dialysis to remove excess chelator, resulted in a MBP-AHL lactonase with greatly decreased activity and metal content. This protein preparation had the same mobility on SDS−PAGE gels but had a different mobility on native PAGE (Figure 3) and was found to elute from a DEAE column at a different conductivity that now matched that of the second, inactive peak described above (~26 mS/cm) and not at the conductivity where it was originally purified. A similar shift is also observed with apo and metal-bound forms of untagged AHL lactonase, although the bands on native PAGE gels are more diffuse, probably due to increased diffusion of this smaller protein (data not shown). The different behavior of apo and metal-bound MBP-AHL lactonase on DEAE columns is useful for purification and was used here to separate apoprotein from any remaining metal-bound protein when purifying the apoprotein for further study. After a final dialysis step to remove NaCl and any remaining *o*-phenanthroline, apo MBP-AHL lactonase was determined to contain only 0.1 equiv of zinc per protein monomer (Table 1). This apoprotein was shown to elute from the DEAE column at the same conductivity as the second, inactive peak (data not shown) and to have the same mobility as the second, inactive peak on native PAGE gels but clearly shows the same mobility as MBP-AHL lactonase that contains 2 equiv of zinc when run on denaturing SDS−PAGE gels (Figure 3). These results and N-terminal sequencing (see above) are consistent with assigning the first peak that elutes from the DEAE column as metal-bound MBP-AHL lactonase and the second as inactive apoprotein. Apoprotein was somewhat less stable than metal-bound lactonase. Frozen stocks of apoprotein showed some protein precipitation, and prolonged incubations of apoprotein resulted in the appearance of some minor degradation products (data not shown).

Reconstitution of Apo MBP-AHL Lactonase with Zinc. To reincorporate zinc, apo MBP-AHL lactonase was dialyzed against $ZnSO_4$ (2 mM), and then excess $ZnSO_4$ was removed by a second dialysis step. To separate any remaining apoprotein from metal-bound protein, the reconstitution mixture was chromatographed on a DEAE column. Apoprotein was originally purified from a peak eluting near 26 mS/cm, but after reconstitution with zinc, a new peak eluted near 19 mS, the same conductivity where the MBP-AHL lactonase containing 2 equiv of zinc elutes. Protein in this new peak also had the same mobility as the 2 equiv zinc-containing MBP-AHL lactonase on native and SDS−PAGE gels, and metal analysis revealed that it now contained 2.5 equiv of zinc per protein monomer (Table 1). Based on A_{280} peak volumes, reconstitution experiments using these conditions result in only ~60% of active enzyme, and the remaining protein elutes from the DEAE column in the flow-through or near 26 mS/cm, where apoprotein elutes. These results indicate that zinc-bound MBP-AHL lactonase can be reconstituted from apoprotein and $ZnSO_4$. However, under these conditions the incorporation is not a high-yield process, so any remaining apoprotein must be removed before characterization of the reconstituted metalloprotein is completed. This was accomplished using DEAE anion-exchange chromatography as described above.

Characterization of the Reaction Products of AHL Lactonase. Control incubation mixtures containing racemic C6-HSL but omitting enzyme showed a $MH^+_{obs} = 200.1 \pm 0.3$

Table 2: EXAFS Curve Fitting Results for Dizinc MBP-AHL Lactonase[a]

fit	scatterer[b]	path[c]	R_{as} (Å)	σ_{as}^{2} [d]	R^e	R^f
1	5 N/O		2.03	7.0	31	189
2	5 N/O		2.03	6.9	89	106
	2 His	C_1	2.92	5.2		
		C_1-N_1	3.14	0.4		
		C_2-N_1	4.21	20		
		$C_1-N_2-N_1$	4.45	14		
3	5 N/O		2.03	7.0	34	51
	2 His	C_1	2.96	7.2		
		C_1-N_1	3.25	8.3		
		C_2-N_1	4.15	12		
		$C_1-N_2-N_1$	4.48	18		
	1 Zn		3.32	6.7		

[a] Values of R_{as} and σ_{as}^2 are for fits to filtered data [$\Delta k = 1-12.5$ Å^{-1}; $\Delta R = 0.8-2.0$ Å (fit 1) or $0.1-4.5$ Å (fits 2 and 3)]. [b] Integer coordination number giving the best fit. [c] Multiple scattering paths represent the combined paths described in Materials and Methods. The labels indicate the individual path with largest amplitude, of those included in the combined path. [d] Mean square deviation in absorber−scatterer bond length in 10^{-3} Å^2. [e] Goodness of fit (R) defined as $1000(\sum_{i=1}^{N}\{[\mathrm{Re}(\chi_{i_{calc}})]^2 + [\mathrm{Im}(\chi_{i_{calc}})]^2\}/\sum_{i=1}^{N}\{[\mathrm{Re}(\chi_{i_{obs}})]^2 + [\mathrm{Im}(\chi_{i_{obs}})]^2\})$, where N is the number of data points for fits to filtered data. [f] Goodness of fit (as defined above) for the same fit to unfiltered data.

peak by ESI-MS, corresponding to the $MH^+_{calc} = 200.12$ for substrate. Incubation mixtures including zinc-containing AHL lactonase showed a new peak at $MH^+_{obs} = 218.2 \pm 0.3$, corresponding to $MH^+_{calc} = 218.13$ for the ring-opened product, *N*-hexanoylhomoserine, as well as retaining a peak at $MH^+_{obs} = 200.2 \pm 0.3$, probably corresponding to the unhydrolyzed (*R*) enantiomer (see below). This experiment confirmed that the expected *N*-acylhomoserine product was produced (Scheme 1) and showed that the AHL lactonase from *B. thuringiensis* hydrolyzes the lactone, like other AHL lactonases, and does not hydrolyze the amide bond of the substrate like some quorum-quenching enzymes (*30*).

Steady-State Kinetic Parameters of AHL Lactonase Variants. The MBP-AHL lactonase containing 2 equiv of zinc has k_{cat} and K_M values almost indistinguishable from those of untagged AHL lactonase, indicating that the N-terminal MBP fusion does not adversely affect activity (Table 1). Apo MBP-AHL lactonase contains 0.1 equiv of zinc, and this apoprotein shows <3% of the activity of the enzyme that contains 2 equiv of zinc, clearly indicating that removal of the metal ions results in loss of activity (Table 1). Apoprotein that was reconstituted to make MBP-AHL lactonase that contains 2 equiv of zinc regained 70% of its original activity, as assessed by k_{cat}, and had an indistinguishable K_M value (Table 1). These results clearly indicate that metal ions are essential for forming an active AHL lactonase. Assays including C6-(*R*)-HSL at concentrations between 0.05 and 20 mM indicated that hydrolysis of this enantiomer was not catalyzed by the *B. thuringiensis* AHL lactonase.

X-ray Absorption Spectroscopy. EXAFS curve fitting results for MBP-AHL lactonase containing 2 equiv of zinc are summarized in Table 2. EXAFS, $k^3\chi(k)$, data, and corresponding Fourier transforms are presented in Figure 4. Single-scattering fits to Fourier-filtered first-shell data show an average of 5 N/O donors per zinc ion, at a distance of 2.03 Å (Table 2). Distinct shells of nitrogen and oxygen first-shell donors could not be defined with the current data (ΔR, 0.13 Å); inclusion of sulfur in first-shell fits resulted in an increase in the fit residual. Multiple-scattering fits, presented

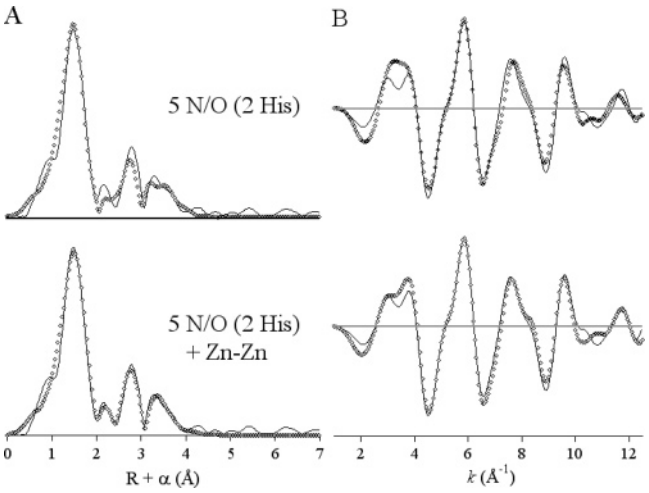

FIGURE 4: Fourier transforms (A) of experimental k^3-weighted EXAFS data (B) for MBP-AHL lactonase containing 2 equiv of zinc (black lines) and best fits (open diamonds). (Top) Multiple scattering fit including two histidine imidazoles, among five total N/O donors per zinc ion. (Bottom) Multiple scattering fit of five N/O donors, including two histidine imidazoles, per zinc ion, and including a Zn−Zn interaction at 3.32 Å. Data are presented on the same scale, offset vertically for clarity.

as the sum of 5 N/O donors including two rigid imidazole ligands (Figure 4, top), indicate an average of 2 ± 0.5 histidine ligands per zinc ion. The increasing values of σ_{as}^2 for the longer multiple-scattering paths (Table 2) are consistent with the greater spread in the (i) number of scattering legs and (ii) overall length of individual paths included in each of the "combined" paths used to model imidazole scattering, as described above.

The multiple-scattering fit (Figure 4A, top; fit 2 in Table 2) adequately reproduces the intensity pattern of the outer-shell scattering, with the exception of a slightly offset center of gravity in the most intense feature ($R + \alpha \approx 2.8$ Å) and an unresolved splitting of the outermost feature. Closer inspection of the *k*-space data (Figure 4B, top) reveals these discrepancies as a missing frequency component, most apparent in the unduplicated splitting of the first full oscillation ($k \approx 3.4$) and a small phase shift in the third and fifth oscillations. This missing component could be modeled with a distant shell of carbon atoms. However, a chemically unreasonable coordination number of 4−6 such interactions per zinc ion was required to achieve only minor improvement in the fit quality. In contrast, inclusion of a single Zn−Zn interaction resulted in a markedly better fit (Figure 4, bottom), reproducing all of the zero crossings in the data, the splitting at $k \approx 3.4$ and the shoulder at $k \approx 8.3$. The metal−metal vector modestly increases the number of variable parameters, from 10 (Figure 4, top; fit 2) to 12 (Figure 4, bottom; fit 3). Given the complexity of the overall fit, the reduction in fit residual upon inclusion of the metal−metal interaction (62%, Table 2) is dramatic and provides strong evidence for a dinuclear zinc active site in the AHL lactonase that contains 2 equiv of zinc.

DISCUSSION

The AHL lactonases have significant potential for use in disrupting the quorum-sensing dependent processes of pathogenic organisms (*6*). However, the catalytic mechanisms of these enzymes have not been established. To produce

recombinant AHL lactonase for detailed studies, the coding sequence of the AHL lactonase from *B. thuringiensis* was cloned from genomic DNA. Previous studies have reported the expression of AHL lactonase as a fusion protein to glutathione *S*-transferase (*12*). However, to avoid any potential complications of glutathione ligation to active site metals, the *B. thuringiensis* AHL lactonase was cloned and expressed as a fusion protein using maltose-binding protein as the N-terminal tag (Figure 1). Purification of this fusion protein by affinity chromatography resulted in a mixture of two major species detected by native gels but indistinguishable by SDS−PAGE gels (Figure 3). These two components could be separated by DEAE anion-exchange chromatography and correspond to active metal-bound MBP-AHL lactonase and inactive apo MBP-AHL lactonase (Figure 2). A change in protein mobility on native gels after removal of bound metal ions is not unprecedented (*31*). Here, the differing properties of apo and metal-bound lactonase were used to prepare purified apoprotein and purified metal-bound protein for further study.

Analysis of the reaction products after incubation of racemic C6-HSL with AHL lactonase confirms that this enzyme is active and that it hydrolyzes the lactone and not the amide bond of the substrate, as expected. All of the reported naturally occurring AHL signals to date have an (*S*) chiral center, reflecting the chirality of its *S*-adenosylmethionine bioprecursor (*32*). To gain more information about the stereochemical constraints of the AHL lactonase active site, the nonnatural (*R*) enantiomer of C6-HSL (**2**) was synthesized, tested as a substrate, and found to be resistant to hydrolysis by the *B. thuringiensis* AHL lactonase. These results add to our understanding of the AHL lactonases by demonstrating that the active site seems to have been optimized for processing the naturally occurring (*S*)-AHL enantiomers and supports the idea that these lactonases have evolved as quorum-quenching enzymes with specificity for AHLs.

The AHL lactonases from two bacterial sources can now be compared kinetically. The k_{cat} for C6-(*S*)-HSL (**1**) hydrolysis by the *B. thuringiensis* lactonase is >3 times faster than that of the *Bacillus* sp. 240B1 enzyme (*12*), but the sequence difference between these enzymes precludes the use of this comparison to directly determine the relative amounts of active protein found in each preparation. The K_M values for C6-(*S*)-HSL (**1**) are similar, differing only by 1.7-fold (*12*). In general, the millimolar K_M values reported for AHL lactonases are somewhat higher than the low micromolar concentrations of AHLs reported for the culture media of some quorum-sensing organisms (*33*, *34*). However, the identity and concentration of AHLs encountered by the *Bacillus* lactonases in nature have not yet been well defined. For example, concentrations of AHLs produced in some biofilms can actually be much higher than those found in laboratory broth cultures, even approaching millimolar concentrations (*35*).

Metal-bound MBP-AHL lactonase was found to tightly bind 1.6 mol of zinc per mol of protein monomer, suggesting that this protein may be able to bind a total of 2 equiv of metal (Table 1). To prepare a uniform metalloprotein suitable for quantitative analysis, additional $ZnSO_4$ was included in the culture media, and the amount of protein found in the active metal-bound peak was observed to increase (Figure 2). Using these expression conditions, purified AHL lactonase is shown to tightly bind 2.3 equiv of zinc (Table 1). Specific proteolysis and subsequent removal of the N-terminal maltose-binding fusion protein resulted in an untagged AHL lactonase that displays similar kinetics to the fusion protein and still binds 1.7 equiv of zinc, indicating that these two metal ions are bound to AHL lactonase and not to the maltose-binding protein. The evidence presented here clearly indicates that the AHL lactonase from *B. thuringiensis* is isolated as a metalloprotein and that the form of this enzyme containing 2 equiv of zinc is an active catalyst of AHL hydrolysis. The loss of catalytic activity upon removal of zinc and the ability to regain activity after reincorporation of zinc into apoprotein show that these metal ions are essential for forming an active enzyme. Further studies will be required to determine if both metal ions are essential and whether AHL lactonase is strictly a zinc protein like the putative phosphodiesterase ZiPD (*36*) or if it is active with alternative metals bound, like glyoxalase II from *Arabidopsis*, which is thought to contain a mixed zinc/iron dinuclear site (*37*).

Our finding that *B. thuringiensis* AHL lactonase is a metalloprotein sharply contrasts with an earlier study of the AHL lactonase from *Bacillus* sp. 240B1 (*12*). These two lactonases share over 90% amino acid identity. However, the AHL lactonase from *Bacillus* sp. 240B1 reportedly does *not* require metal ions for catalysis, a conclusion based in part on observations that the protein only contained 0.08 equiv of zinc; short incubation periods with metal ions and chelators do not significantly alter its activity, and mutations of proposed zinc ligands do not result in total loss of activity (*12*). Although the sequences of the AHL lactonases from these two sources differ at 24 out of 250 total residues, the seven proposed zinc ligands (see below) are absolutely conserved. Some of our experimental observations may help to explain the apparent differences in metal content found between these two proteins. In our studies, affinity chromatography was only able to resolve MBP fusion proteins from nonfusion proteins and was not able to separate metal-bound from apo MBP-AHL lactonase. If no further purification steps are taken after an affinity column, as is the case for the lactonase from *Bacillus* sp. 240B1 (*12*), it is possible that active metalloprotein is contaminated with inactive apoprotein. This contamination would not be detected by SDS−PAGE because these two proteins have the same mobility and would lead to an artifactually low zinc to protein ratio. In addition, our experience indicates that short incubation periods with chelators or alternative metals are not very effective in significantly changing the metal content of zinc-bound protein or apoprotein. Although earlier reports have shown that mutation of one (or more) of these putative metal binding residues in AHL lactonase does not abolish catalytic activity (*12*), more rigorous characterization will be required to determine whether these mutations are sufficient to eliminate zinc binding. Of course, the possibility still exists that the minor amino acid differences between these two proteins could account for their differing metal content, but this seems unlikely. The sequence similarity, the precedence of other superfamily members, and the results of this current study all support the identification of AHL lactonase as a metalloprotein that requires metal ions for catalytic activity.

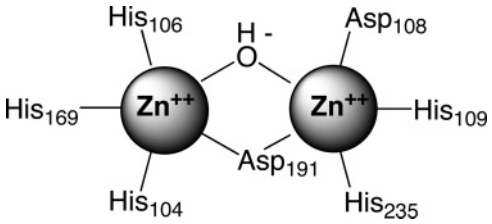

FIGURE 5: Proposed dinuclear metal binding site containing 2 equiv of zinc.

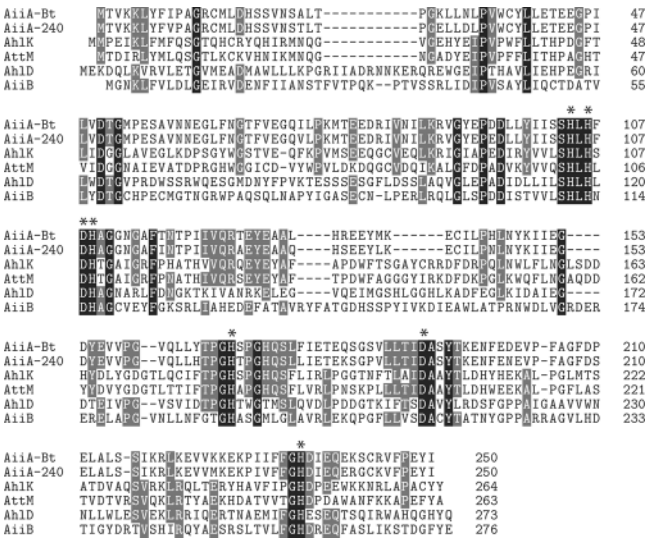

FIGURE 6: Protein sequence alignment of various AHL lactonases. Sequences of AHL lactonases with experimentally demonstrated activity from *B. thuringiensis* subsp. kurstaki (AiiA-Bt), *Bacillus* sp. 240B1 (AiiA-240) (*12*), *Klebsiella pneumoniae* KCTC2241 (AhlK) (*45*), *Arthrobacter* sp. IBN110 (AhlD) (*45*), and *Agrobacterium tumefaciens* (AttM and AiiB) (*46*, *47*) were aligned using Clustal W (*48*), and TeXshade (*49*) was used to shade identical residues with black and conserved residues with gray. An asterisk marks proposed metal ligands for the dinuclear zinc form of AHL lactonase.

X-ray absorption spectroscopy was used to probe the local environment of the bound metal ions in MBP-AHL lactonase containing 2 equiv of zinc. Fits to the EXAFS data indicate an average of five N/O ligands, including 2 ± 0.5 histidines, per zinc ion, and are consistent with the two zinc ions binding as a dinuclear site. These spectroscopic data can be combined with sequence alignments of known AHL lactonases to build a proposed model of this dinuclear zinc binding site (Figure 5). Comparison of AHL lactonase with other superfamily members including glyoxalase II (*38*), ZiPD (*39*), and methyl parathion hydrolase (*40*), suggests possible zinc binding residues which are totally conserved in all known AHL lactonases: His104, His106, and His169 for the metal-1 site and Asp108, His109, and His235 for the metal-2 site (Figure 6). In the other superfamily members that contain these metal binding ligands, one oxygen atom of Asp191 and a water molecule (presumably a hydroxide) bridge the two metal ions. This proposed model is also consistent with the information derived from the current EXAFS data. The determination of an average 5 ± 1 nitrogen or oxygen neighbors to each zinc atom matches the proposed metal-1 and metal-2 sites, which are both five coordinate, with all nitrogen and oxygen ligands. The average number of 2 ± 0.5 histidine ligands per zinc ion is also consistent with this model in which three histidine residues ligate metal 1 and two ligate metal 2. The zinc−zinc distance determined for dinuclear zinc AHL lactonase of 3.32 Å is very similar to the 3.3−3.5 Å distance reported in a dinuclear zinc human glyoxalase II crystal structure (*38*) and the 3.32 Å for *E. coli* ZiPD determined by EXAFS (*39*).

The metallo-*β*-lactamase superfamily contains enzymes that show considerable variation in the ligands, specificity, and stoichiometry of its metal cofactors. Other superfamily members containing the same seven proposed metal binding residues as AHL lactonase include the following: glyoxalase II, a thioesterase that has been shown to harbor a dinuclear zinc (*38*) or a zinc/iron dinuclear site (*37*); ZiPD, a phosphodiesterase that is active with a dinuclear zinc site (*39*); and methyl parathion hydrolase, for which structural coordinates of the dinuclear zinc and zinc/cadmium proteins have been deposited (*40*). This study now adds an additional enzymic activity to those catalyzed by glyoxalase II-like active sites: hydrolysis of AHLs. Considering the Lewis acidity of each metal and the nucleophilicity of a bound hydroxide, the metal binding sites found in this superfamily of enzymes provide considerable functionality in a compact space and have been exploited by nature to evolve different solutions to a diverse set of catalytic challenges. For example, just the hydrolytic enzymes found in this superfamily use at least three different mechanisms for catalysis (*36*, *38*, *41*−*44*). Although conceptual parallels can be drawn, this diversity necessitates further study to determine exactly how AHL lactonase uses its metal ions to catalyze the degradation of these quorum-sensing signal molecules. To our knowledge, this is the first evidence that the quorum-quenching AHL lactonase from *B. thuringiensis* is a stereoselective metalloprotein in which two metal ions, required for catalytic activity, bind in close proximity forming a dinuclear site. Detailed knowledge of the metal binding site in AHL lactonase is essential for optimizing the use of this family of enzymes as quorum-quenching agents, adds an additional catalytic activity to those known to be catalyzed by glyoxalase II-like active sites, and also increases our understanding of the metal binding properties found in the metallo-*β*-lactamase superfamily.

ACKNOWLEDGMENT

We thank Terezie H. Schaller for assistance in cloning wild-type AHL lactonase, Helena Bianchi for assistance with purifying AHL lactonase, Jessica Momb for assistance with C6-(*S*)-HSL synthesis, and John M. Lansdown for assistance with the metal analysis.

REFERENCES

1. Fuqua, C., Parsek, M. R., and Greenberg, E. P. (2001) Regulation of gene expression by cell-to-cell communication: acyl-homoserine lactone quorum sensing, *Annu. Rev. Genet. 35*, 439−468.
2. Miller, M. B., and Bassler, B. L. (2001) Quorum sensing in bacteria, *Annu. Rev. Microbiol. 55*, 165−199.
3. Smith, R. S., and Iglewski, B. H. (2003) *P. aeruginosa* quorum-sensing systems and virulence, *Curr. Opin. Microbiol. 6*, 56−60.
4. Von Bodman, S. B., Bauer, W. D., and Coplin, D. L. (2003) Quorum sensing in plant-pathogenic bacteria, *Annu. Rev. Phytopathol. 41*, 455−482.
5. Ulrich, R. L., Deshazer, D., Hines, H. B., and Jeddeloh, J. A. (2004) Quorum sensing: a transcriptional regulatory system involved in the pathogenicity of *Burkholderia mallei*, *Infect. Immun. 72*, 6589−6596.

6. Zhang, L. H. (2003) Quorum quenching and proactive host defense, *Trends Plant Sci. 8*, 238−244.
7. Reimmann, C., Ginet, N., Michel, L., Keel, C., Michaux, P., Krishnapillai, V., Zala, M., Heurlier, K., Triandafillu, K., Harms, H., Defago, G., and Haas, D. (2002) Genetically programmed autoinducer destruction reduces virulence gene expression and swarming motility in *Pseudomonas aeruginosa* PAO1, *Microbiology 148*, 923−932.
8. Dong, Y. H., Wang, L. H., Xu, J. L., Zhang, H. B., Zhang, X. F., and Zhang, L. H. (2001) Quenching quorum-sensing-dependent bacterial infection by an *N*-acyl homoserine lactonase, *Nature 411*, 813−817.
9. Ulrich, R. L. (2004) Quorum quenching: enzymatic disruption of *N*-acylhomoserine lactone-mediated bacterial communication in *Burkholderia thailandensis*, *Appl. Environ. Microbiol. 70*, 6173−6180.
10. Dong, Y. H., Xu, J. L., Li, X. Z., and Zhang, L. H. (2000) AiiA, an enzyme that inactivates the acylhomoserine lactone quorum-sensing signal and attenuates the virulence of *Erwinia carotovora*, *Proc. Natl. Acad. Sci. U.S.A. 97*, 3526−3531.
11. Aravind, L. (1999) An evolutionary classification of the metallo-beta-lactamase fold proteins, *In Silico Biol. 1*, 69−91.
12. Wang, L. H., Weng, L. X., Dong, Y. H., and Zhang, L. H. (2004) Specificity and enzyme kinetics of the quorum-quenching *N*-Acyl homoserine lactone lactonase (AHL-lactonase), *J. Biol. Chem. 279*, 13645−13651.
13. Ausubel, F. M. (1987) *Current protocols in molecular biology*, Greene Publishing Associates, J. Wiley, Brooklyn, NY.
14. Dong, Y. H., Gusti, A. R., Zhang, Q., Xu, J. L., and Zhang, L. H. (2002) Identification of quorum-quenching *N*-acyl homoserine lactonases from *Bacillus* species, *Appl. Environ. Microbiol. 68*, 1754−1759.
15. Kristelly, R., Earnest, B. T., Krishnamoorthy, L., and Tesmer, J. J. (2003) Preliminary structure analysis of the DH/PH domains of leukemia-associated RhoGEF, *Acta Crystallogr., Sect. D: Biol. Crystallogr. 59*, 1859−1862.
16. Kapust, R. B., Tozser, J., Fox, J. D., Anderson, D. E., Cherry, S., Copeland, T. D., and Waugh, D. S. (2001) Tobacco etch virus protease: mechanism of autolysis and rational design of stable mutants with wild-type catalytic proficiency, *Protein Eng. 14*, 993−1000.
17. Laemmli, U. K. (1970) Cleavage of structural proteins during the assembly of the head of bacteriophage T4, *Nature 227*, 680−685.
18. Wang, S. C., Person, M. D., Johnson, W. H., Jr., and Whitman, C. P. (2003) Reactions of *trans*-3-chloroacrylic acid dehalogenase with acetylene substrates: consequences of and evidence for a hydration reaction, *Biochemistry 42*, 8762−8773.
19. Chhabra, S. R., Harty, C., Hooi, D. S., Daykin, M., Williams, P., Telford, G., Pritchard, D. I., and Bycroft, B. W. (2003) Synthetic analogues of the bacterial signal (quorum sensing) molecule *N*-(3-oxododecanoyl)-L-homoserine lactone as immune modulators, *J. Med. Chem. 46*, 97−104.
20. Khalifah, R. G. (1971) The carbon dioxide hydration activity of carbonic anhydrase. I. Stop-flow kinetic studies on the native human isoenzymes B and C, *J. Biol. Chem. 246*, 2561−2573.
21. Hurt, J. D., Tu, C., Laipis, P. J., and Silverman, D. N. (1997) Catalytic properties of murine carbonic anhydrase IV, *J. Biol. Chem. 272*, 13512−13518.
22. Schindler, J. F., Naranjo, P. A., Honaberger, D. A., Chang, C. H., Brainard, J. R., Vanderberg, L. A., and Unkefer, C. J. (1999) Haloalkane dehalogenases: steady-state kinetics and halide inhibition, *Biochemistry 38*, 5772−5778.
23. Stern, E. A. (1993) Number of relevant independent points in X-ray-absorption fine-structure spectra, *Phys. Rev. B 48*, 9825−9827.
24. Ankudinov, A. L., Ravel, B., Rehr, J. J., and Condradson, S. D. (1998) Real space multiple scattering calculation and Interpretation of XANES, *Phys. Rev. B 58*, 7565−7576.
25. McClure, C. P., Rusche, K. M., Peariso, K., Jackman, J. E., Fierke, C. A., and Penner-Hahn, J. E. (2003) EXAFS studies of the zinc sites of UDP-(3-O-acyl)-*N*-acetylglucosamine deacetylase (LpxC), *J. Inorg. Biochem. 94*, 78−85.
26. Lee, S. J., Park, S. Y., Lee, J. J., Yum, D. Y., Koo, B. T., and Lee, J. K. (2002) Genes encoding the *N*-acyl homoserine lactone-degrading enzyme are widespread in many subspecies of *Bacillus thuringiensis*, *Appl. Environ. Microbiol. 68*, 3919−3924.
27. Bradford, M. M. (1976) A rapid and sensitive method for the quantitation of microgram quantities of protein utilizing the principle of protein-dye binding, *Anal. Biochem. 72*, 248−254.
28. Smith, P. K., Krohn, R. I., Hermanson, G. T., Mallia, A. K., Gartner, F. H., Provenzano, M. D., Fujimoto, E. K., Goeke, N. M., Olson, B. J., and Klenk, D. C. (1985) Measurement of protein using bicinchoninic acid, *Anal. Biochem. 150*, 76−85.
29. Gill, S. C., and von Hippel, P. H. (1989) Calculation of protein extinction coefficients from amino acid sequence data, *Anal. Biochem. 182*, 319−326.
30. Lin, Y. H., Xu, J. L., Hu, J., Wang, L. H., Ong, S. L., Leadbetter, J. R., and Zhang, L. H. (2003) Acyl-homoserine lactone acylase from *Ralstonia* strain XJ12B represents a novel and potent class of quorum-quenching enzymes, *Mol. Microbiol. 47*, 849−860.
31. Lyons, T. J., Nersissian, A., Goto, J. J., Zhu, H., Gralla, E. B., and Valentine, J. S. (1998) Metal ion reconstitution studies of yeast copper−zinc superoxide dismutase: the "phantom" subunit and the possible role of Lys7p, *J. Biol. Inorg. Chem. 3*, 650−662.
32. More, M. I., Finger, L. D., Stryker, J. L., Fuqua, C., Eberhard, A., and Winans, S. C. (1996) Enzymatic synthesis of a quorum-sensing autoinducer through use of defined substrates, *Science 272*, 1655−1658.
33. Flagan, S., Ching, W. K., and Leadbetter, J. R. (2003) *Arthrobacter* strain VAI-A utilizes acyl-homoserine lactone inactivation products and stimulates quorum signal biodegradation by *Variovorax paradoxus*, *Appl. Environ. Microbiol. 69*, 909−916.
34. Pearson, J. P., Passador, L., Iglewski, B. H., and Greenberg, E. P. (1995) A second *N*-acylhomoserine lactone signal produced by *Pseudomonas aeruginosa*, *Proc. Natl. Acad. Sci. U.S.A. 92*, 1490−1494.
35. Charlton, T. S., de Nys, R., Netting, A., Kumar, N., Hentzer, M., Givskov, M., and Kjelleberg, S. (2000) A novel and sensitive method for the quantification of *N*-3-oxoacyl homoserine lactones using gas chromatography−mass spectrometry: application to a model bacterial biofilm, *Environ. Microbiol. 2*, 530−541.
36. Vogel, A., Schilling, O., Niecke, M., Bettmer, J., and Meyer-Klaucke, W. (2002) ElaC encodes a novel binuclear zinc phosphodiesterase, *J. Biol. Chem. 277*, 29078−29085.
37. Zang, T. M., Hollman, D. A., Crawford, P. A., Crowder, M. W., and Makaroff, C. A. (2001) *Arabidopsis* glyoxalase II contains a zinc/iron binuclear metal center that is essential for substrate binding and catalysis, *J. Biol. Chem. 276*, 4788−4795.
38. Cameron, A. D., Ridderstrom, M., Olin, B., and Mannervik, B. (1999) Crystal structure of human glyoxalase II and its complex with a glutathione thiolester substrate analogue, *Struct. Folding Des. 7*, 1067−1078.
39. Vogel, A., Schilling, O., and Meyer-Klaucke, W. (2004) Identification of metal binding residues for the binuclear zinc phosphodiesterase reveals identical coordination as glyoxalase II, *Biochemistry 43*, 10379−10386.
40. Sun, L., Dong, Y., Zhou, Y., Yang, M., Zhang, C., Rao, Z., and Zhang, X. E. (2004) Crystallization and preliminary X-ray studies of methyl parathion hydrolase from *Pseudomonas* sp. WBC-3, *Acta Crystallogr., Sect. D: Biol. Crystallogr. 60*, 954−956.
41. Bounaga, S., Laws, A. P., Galleni, M., and Page, M. I. (1998) The mechanism of catalysis and the inhibition of the *Bacillus cereus* zinc-dependent beta-lactamase, *Biochem. J. 331* (Part 3), 703−711.
42. Wang, Z., Fast, W., Valentine, A. M., and Benkovic, S. J. (1999) Metallo-beta-lactamase: structure and mechanism, *Curr. Opin. Chem. Biol. 3*, 614−622.
43. Garau, G., Bebrone, C., Anne, C., Galleni, M., Frere, J. M., and Dideberg, O. (2005) A metallo-beta-lactamase enzyme in action: crystal structures of the monozinc carbapenemase CphA and its complex with biapenem, *J. Mol. Biol. 345*, 785−795.
44. Schilling, O., Wenzel, N., Naylor, M., Vogel, A., Crowder, M., Makaroff, C., and Meyer-Klaucke, W. (2003) Flexible metal binding of the metallo-beta-lactamase domain: glyoxalase II incorporates iron, manganese, and zinc in vivo, *Biochemistry 42*, 11777−11786.
45. Park, S. Y., Lee, S. J., Oh, T. K., Oh, J. W., Koo, B. T., Yum, D. Y., and Lee, J. K. (2003) AhlD, an N-acylhomoserine lactonase in *Arthrobacter* sp., and predicted homologues in other bacteria, *Microbiology 149*, 1541−1550.
46. Zhang, H. B., Wang, L. H., and Zhang, L. H. (2002) Genetic control of quorum-sensing signal turnover in *Agrobacterium tumefaciens*, *Proc. Natl. Acad. Sci. U.S.A. 99*, 4638−4643.

47. Carlier, A., Uroz, S., Smadja, B., Fray, R., Latour, X., Dessaux, Y., and Faure, D. (2003) The Ti plasmid of *Agrobacterium tumefaciens* harbors an attM-paralogous gene, aiiB, also encoding *N*-Acyl homoserine lactonase activity, *Appl. Environ. Microbiol. 69*, 4989−4993.
48. Thompson, J. D., Higgins, D. G., and Gibson, T. J. (1994) CLUSTAL W: improving the sensitivity of progressive multiple sequence alignment through sequence weighting, position-specific gap penalties and weight matrix choice, *Nucleic Acids Res. 22*, 4673−4680.
49. Beitz, E. (2000) TEXshade: shading and labeling of multiple sequence alignments using LATEX2 epsilon, *Bioinformatics 16*, 135−139.

BI050050M